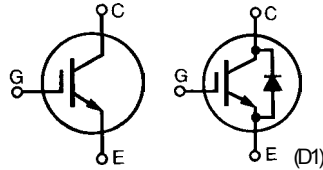


HiPerFAST™ IGBT

IXGH39N60B
IXGH39N60BD1
IXGT39N60B
IXGT39N60BD1

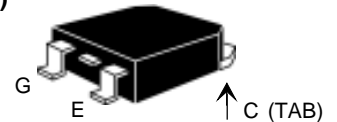
$V_{CES} = 600 \text{ V}$
 $I_{C25} = 76 \text{ A}$
 $V_{CE(sat)} = 1.7 \text{ V}$
 $t_{fi} = 200 \text{ ns}$

Preliminary data

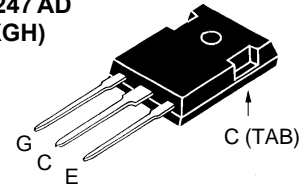


Symbol	Test Conditions	Maximum Ratings	
V_{CES}	$T_J = 25^\circ\text{C to } 150^\circ\text{C}$	600	V
V_{CGR}	$T_J = 25^\circ\text{C to } 150^\circ\text{C}; R_{GE} = 1 \text{ M}\Omega$	600	V
V_{GES}	Continuous	± 20	V
V_{GEM}	Transient	± 30	V
I_{C25}	$T_C = 25^\circ\text{C}$	76	A
I_{C90}	$T_C = 90^\circ\text{C}$	39	A
I_{CM}	$T_C = 25^\circ\text{C}, 1 \text{ ms}$	152	A
SSOA (RBSOA)	$V_{GE} = 15 \text{ V}, T_{VJ} = 125^\circ\text{C}, R_G = 22 \Omega$ Clamped inductive load	$I_{CM} = 76$ @ $0.8 V_{CES}$	A
P_C	$T_C = 25^\circ\text{C}$	200	W
T_J		-55 ... +150	$^\circ\text{C}$
T_{JM}		150	$^\circ\text{C}$
T_{stg}		-55 ... +150	$^\circ\text{C}$
Maximum lead temperature for soldering 1.6 mm (0.062 in.) from case for 10 s		300	$^\circ\text{C}$
M_d	Mounting torque (M3) TO-247	1.13/10Nm/lb.in.	
Weight		TO-247 AD	6 g
		TO-268	4 g

TO-268
(IXGT)



TO-247 AD
(IXGH)



G = Gate, C = Collector,
E = Emitter, TAB = Collector

Features

- International standard packages JEDEC TO-247 AD & TO-268
- High current handling capability
- Newest generation HDMOS™ process
- MOS Gate turn-on - drive simplicity

Applications

- PFC circuits
- AC motor speed control
- DC servo and robot drives
- DC choppers
- Uninterruptible power supplies (UPS)
- Switched-mode and resonant-mode power supplies

Advantages

- High power density
- Very fast switching speeds for high frequency applications

Symbol	Test Conditions		Characteristic Values ($T_J = 25^\circ\text{C}$, unless otherwise specified)		
			Min.	Typ.	Max.
BV_{CES}	$I_C = 250 \mu\text{A}, V_{GE} = 0 \text{ V}$	39N60B	600		V
		39N60BD1	600		
$V_{GE(th)}$	$I_C = 250 \mu\text{A}, V_{CE} = V_{GE}$	39N60B	2.5		5.0 V
		39N60BD1	2.5		5.0 V
I_{CES}	$V_{CE} = 0.8 \cdot V_{CES}, V_{GE} = 0 \text{ V}$	$T_J = 25^\circ\text{C}$ 39N60B			200 μA
		$T_J = 125^\circ\text{C}$ 39N60B			1 mA
		$T_J = 125^\circ\text{C}$ 39N60BD1			3 mA
I_{GES}	$V_{CE} = 0 \text{ V}, V_{GE} = \pm 20 \text{ V}$				$\pm 100 \text{ nA}$
$V_{CE(sat)}$	$I_C = I_{90}, V_{GE} = 15 \text{ V}$				1.7 V

Fig. 1. Saturation Voltage Characteristics @ 25 Deg. C

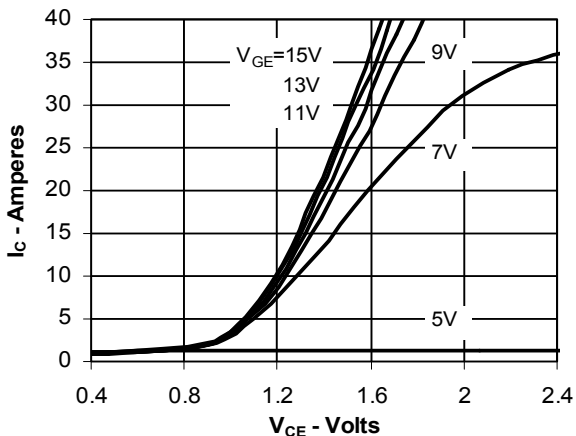


Fig. 2. Extended Output Characteristics @ 25 Deg. C

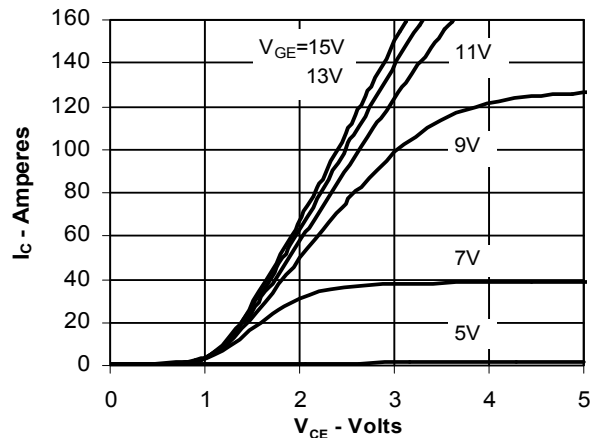


Fig. 3. Saturation Voltage Characteristics @ 125 Deg. C

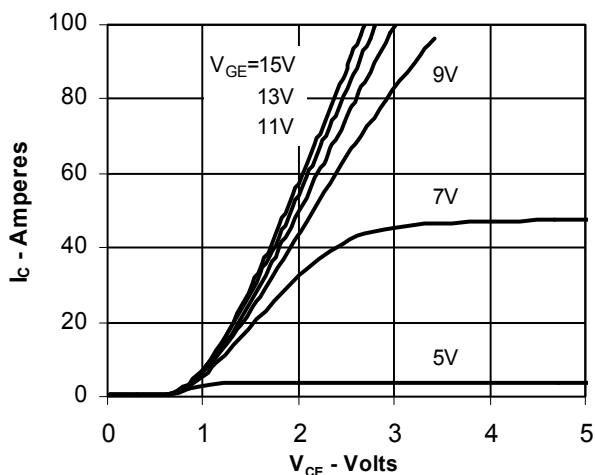


Fig. 4. Temperature Dependence of $V_{CE(SAT)}$

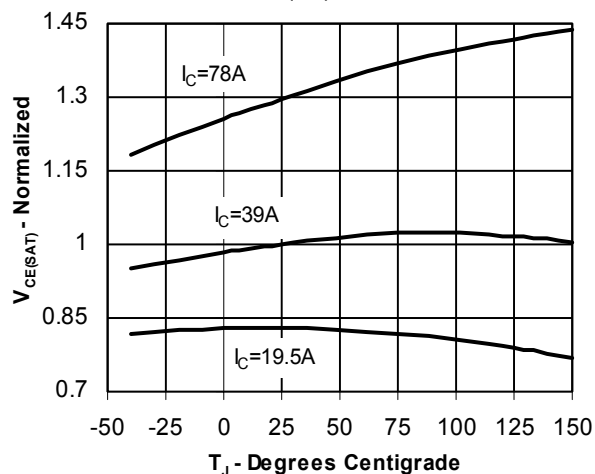


Fig. 5. BV_{CES} & $V_{(GE)TH}$ vs. Junction Temperature

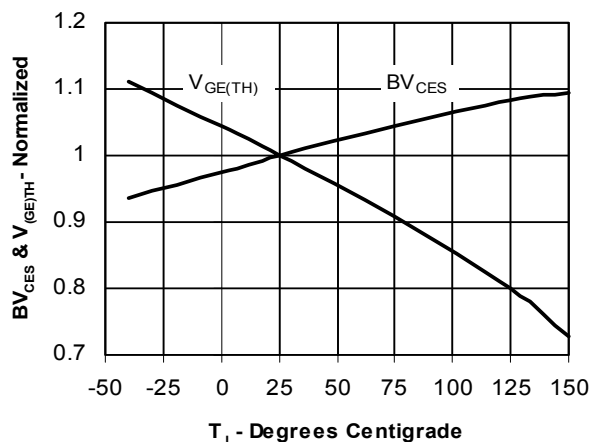


Fig. 6. Admittance

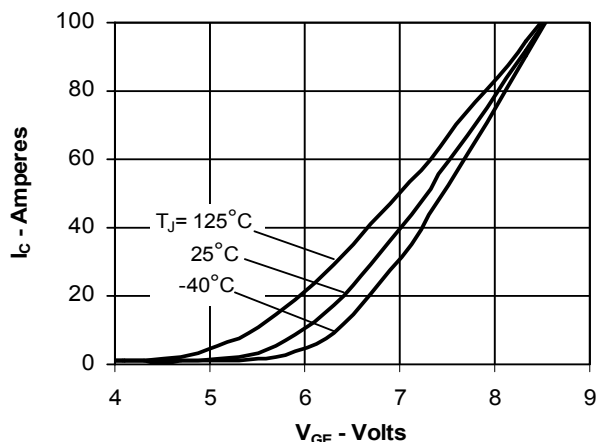


Fig. 7. Transconductance

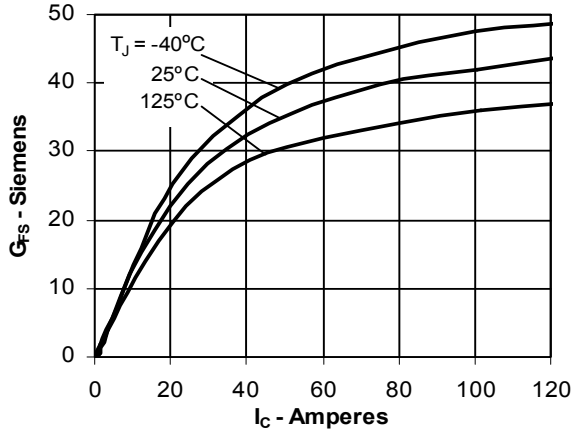


Fig. 8. Dependence of E_{OFF} on I_c

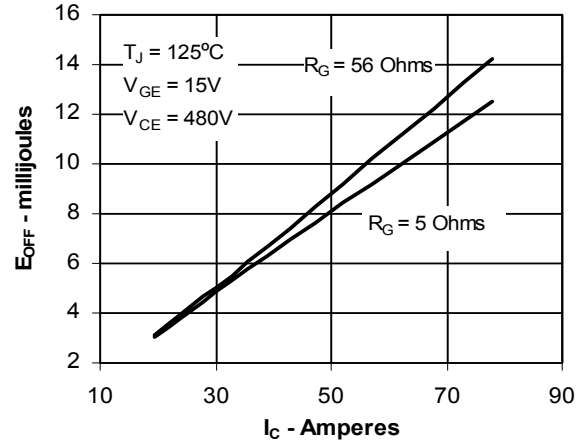


Fig. 9. Dependence of E_{OFF} on R_G

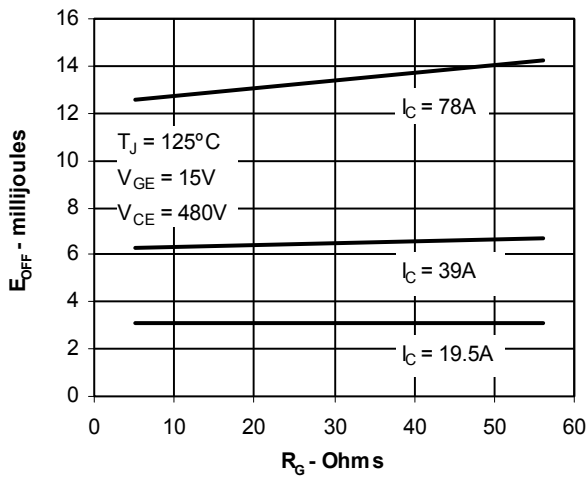


Fig. 10. Dependence of E_{OFF} on Temperature

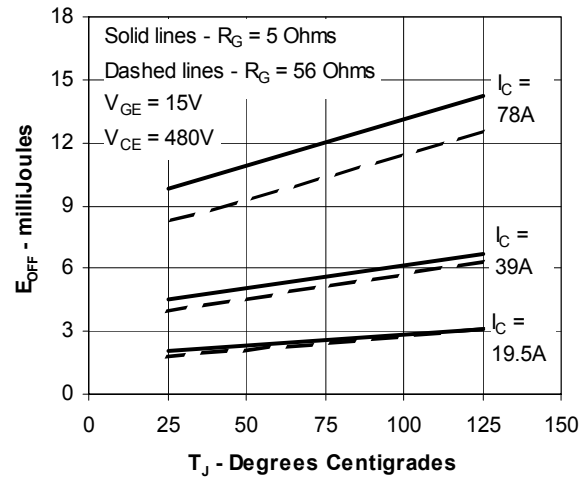


Fig. 11. Gate Charge

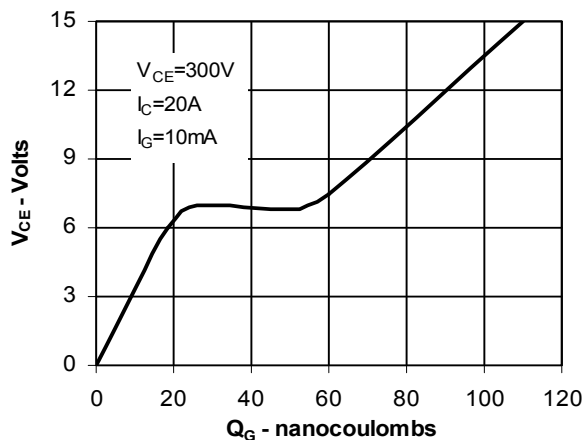
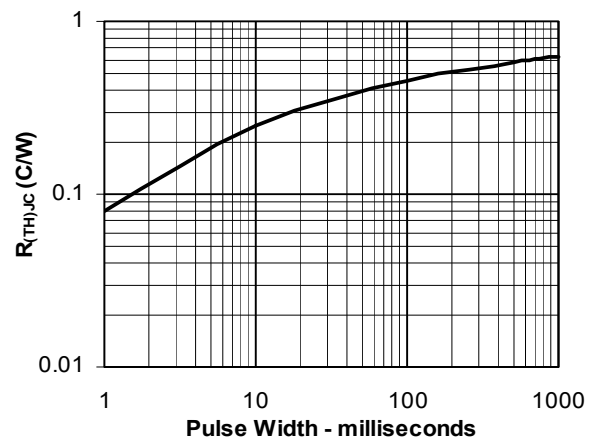


Fig. 12. Transient Thermal Response



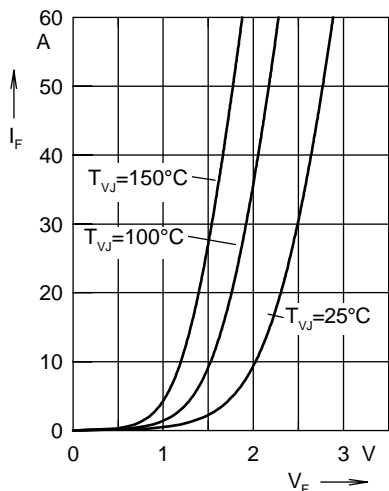


Fig. 12 Forward current I_F versus V_F

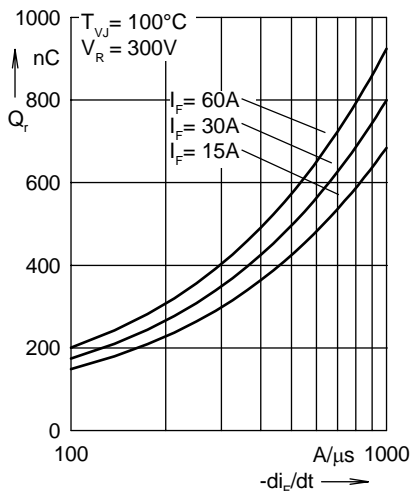


Fig. 13 Reverse recovery charge Q_r versus $-di_F/dt$

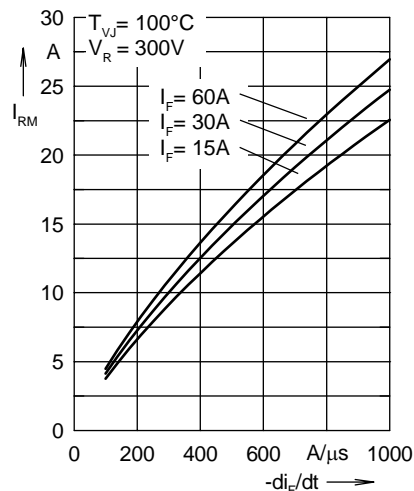


Fig. 14 Peak reverse current I_{RM} versus $-di_F/dt$

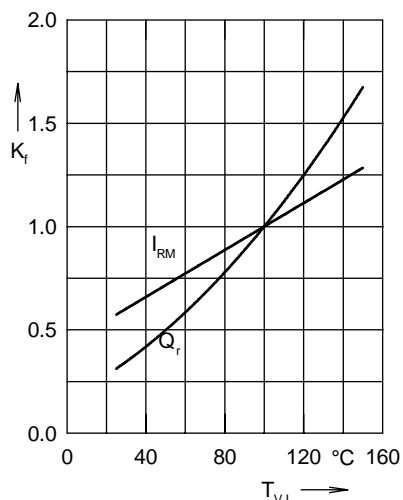


Fig. 15 Dynamic parameters Q_r, I_{RM} versus T_{VJ}

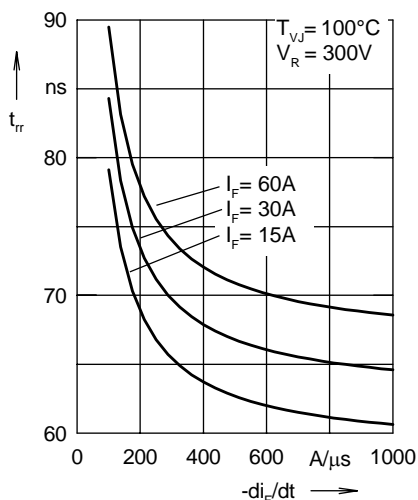


Fig. 16 Recovery time t_{rr} versus $-di_F/dt$

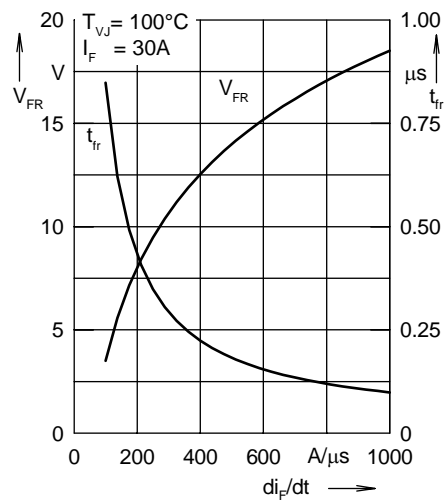


Fig. 17 Peak forward voltage V_{FR} and t_{rr} versus di_F/dt

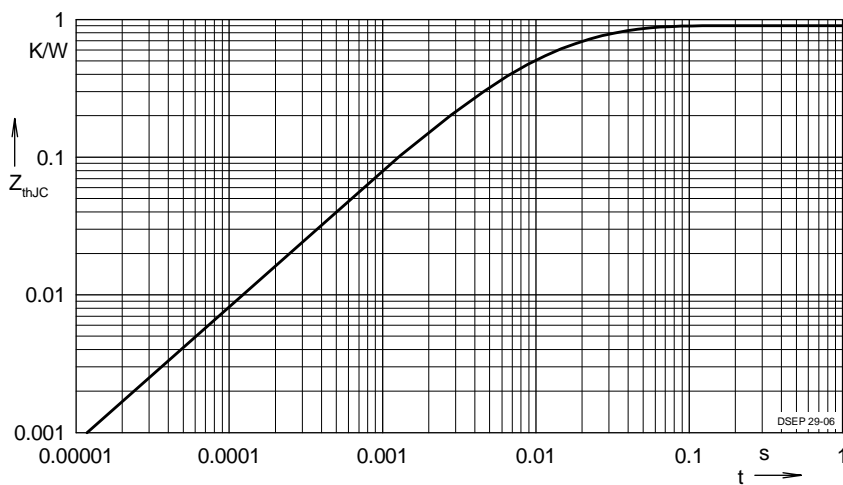


Fig. 18 Transient thermal resistance junction to case

Constants for Z_{thJC} calculation:

i	R_{thi} (K/W)	t_i (s)
1	0.502	0.0052
2	0.193	0.0003
3	0.205	0.0162